Response of Jakobshavn Isbræ, Greenland, to Holocene climate change

Nicolás E. Young[1]*, Jason P. Briner[1], Heather A.M. Stewart[1], Yarrow Axford[2], Beata Csatho[1], Dylan H. Rood[3,4], and Robert C. Finkel[5]

[1]Department of Geology, University at Buffalo, 411 Cooke Hall, Buffalo, New York 14260, USA
[2]Department of Earth and Planetary Sciences, Northwestern University, 1850 Campus Drive, Evanston, Illinois 60208, USA
[3]Center for Accelerator Mass Spectrometry, Lawrence Livermore National Laboratory, Livermore, California 94550, USA
[4]Department of Earth Science, University of California–Santa Barbara, Santa Barbara, California 93106, USA
[5]Department of Earth and Planetary Sciences, University of California–Berkeley, Berkeley, California 94720, USA

ABSTRACT

Rapid fluctuations in the velocity of Greenland Ice Sheet (GIS) outlet glaciers over the past decade have made it difficult to extrapolate ice-sheet change into the future. This significant short-term variability highlights the need for geologic records of preinstrumental GIS margin fluctuations in order to better predict future GIS response to climate change. Using ^{10}Be surface exposure ages and radiocarbon-dated lake sediments, we constructed a detailed chronology of ice-margin fluctuations over the past 10 k.y. for Jakobshavn Isbræ, Greenland's largest outlet glacier. In addition, we present new estimates of corresponding local temperature changes using a continuous record of insect (Chironomidae) remains preserved in lake sediments. We find that following an early Holocene advance just prior to 8 ka, Jakobshavn Isbræ retreated rapidly at a rate of ~100 m yr^{-1}, likely in response to increasing regional and local temperatures. Ice remained behind its present margin for ~7 k.y. during a warm period in the middle Holocene with sustained temperatures ~2 °C warmer than today, then the land-based margin advanced at least 2–4 km between A.D. 1500–1640 and A.D. 1850. The ice margin near Jakobshavn thus underwent large and rapid adjustments in response to relatively modest centennial-scale Holocene temperature changes, which may foreshadow GIS response to future warming.

INTRODUCTION

The Greenland Ice Sheet (GIS) is by far the largest ice mass in the Arctic, representing a total sea-level equivalent of ~7 m (Alley et al., 2005). Ice discharge via marine-terminating outlet glaciers connected to the GIS interior currently accounts for ~50% of overall GIS mass loss, and projections of GIS contribution to sea-level rise by A.D. 2100 range from ~5–15 cm to ~50 cm (Pfeffer et al., 2008; van den Brooke et al., 2009; Long, 2009). This large range in sea-level rise estimates is due to the limited understanding of dynamic thinning of outlet glaciers (Pritchard et al., 2009), which may increase the ice sheet's sensitivity to climate warming.

Observations over the past decade show that Jakobshavn Isbræ (Fig. 1), which drains ~6.5% of the GIS area, is one of Greenland's most rapidly changing outlet glaciers, having undergone significant retreat, thinning, and a near doubling in terminus velocity and ice discharge between 1996 and 2005 (Joughin et al., 2004; Rignot and Kanagaratnam, 2006). Overall, the calving terminus has retreated ~35 km since A.D. 1850, including 10 km of retreat between 2000 and 2003 (Joughin et al., 2004; Weidick and Bennike, 2007; Csatho et al., 2008). While retreat and thinning on annual to decadal time scales reflect complex interactions of the calving terminus with local climate, oceanographic changes, and interior drainage (e.g., Holland et al., 2008), longer term variability is broadly synchronous with the instrumental temperature record (Csatho et al., 2008).

Although contemporary observations are critical for understanding the mechanisms driving changes in Greenland's outlet glaciers, geological reconstructions of former outlet glacier change provide insights into ice-margin behavior over longer time scales and during periods that were warmer than present (Kaufman et al., 2004; Briner et al., 2009). Furthermore, whereas the observational record has focused almost exclusively on the calving terminus of the glacier, geological studies can also address changes in the land-terminating ice margin near Jakobshavn Isbræ, thus elucidating broader ice-margin responsiveness to climate change.

JAKOBSHAVN ISBRÆ

Jakobshavn Isfjord is a narrow (6–8 km wide) and deep (~800 m) fjord (Holland et al., 2008) that spans ~50 km between Disko Bugt and the GIS margin at Jakobshavn Isbræ (Fig. 1). In

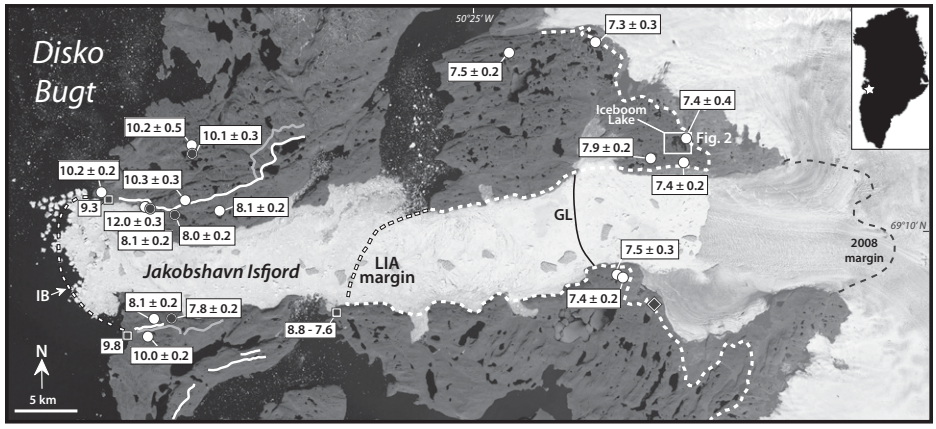

Figure 1. Jakobshavn region showing older (Marrait; gray lines) and younger (Tasiussaq; white lines) Fjord Stade moraines, expressed as Isfjeldsbanken (IB) at the fjord mouth. Also shown is Little Ice Age (LIA) maximum extent (white dashes) and approximate location of LIA grounding line (GL—black line; Csatho et al., 2008). ^{10}Be ages are from bedrock (white dots) and perched erratics (black dots) (in ka; 1 standard deviation, SD). Preexisting radiocarbon ages (cal kyr B.P.) are marked by black squares (Weidick and Bennike, 2007; Long et al., 2006). Marine fauna reworked into LIA moraine (black diamond) are located on south side of Isfjord (Weidick and Bennike, 2007; Table DR3 [see footnote 1]).

*E-mail: nyoung2@buffalo.edu.

addition, the Jakobshavn Isbræ bed is more than 1 km below sea level for at least 70 km inland (Clarke and Echelmeyer, 1996). The ice-free landscape between Disko Bugt and the present ice margin consists of glacially scoured bedrock, erratic boulders, and the prominent Fjord Stade moraine complex (Fig. 1). Prior research provides a general picture of ice-margin changes since the last glaciation. The Isfjord was occupied by Jakobshavn Isbræ during the last glaciation, and became ice free during the Holocene (Weidick and Bennike, 2007). Ice retreated inland from the coastal areas along inner Disko Bugt between ca. 10.3 and 9.3 cal (calibrated) kyr B.P and from the middle Isfjord some time between 8.8 and 7.6 cal kyr B.P. (Long and Roberts, 2003; Long et al., 2006). The age of the widely traceable Fjord Stade moraines (the Marrait moraine and younger Tasiussaq moraine) is loosely constrained between ca. 10 and 7.7 cal kyr B.P. (Weidick and Bennike, 2007). Marine fauna (e.g., bivalves) reworked into the historic moraine on the south side of the Isfjord (Fig. 1) range in age from 6.1 to 3.5 cal kyr B.P., indicating that Jakobshavn Isbræ retreated inland (east) of its present position prior to 6.1 cal kyr B.P., and advanced to its present configuration after 3.5 cal kyr B.P. (Weidick and Bennike, 2007). Holocene temperature reconstructed at Summit Greenland remained above modern values until ca. 4 ka (i.e., Dahl-Jensen et al., 1998), and temperature-driven ice-sheet models support the inference of reduced ice extent during the middle Holocene (Weidick et al., 1990; Simpson et al., 2009). Reconstructions of relative sea-level change from the Disko Bugt region reveal landscape submergence initiating 3–2 cal kyr B.P., which is thought to represent increased ice loading resulting from GIS expansion during Neoglaciation (Long et al., 2006). Marine cores just beyond the fjord mouth suggest that Jakobshavn Isbræ reached late Holocene maxima between A.D. 1200 and 1660 and after A.D. 1450 (Lloyd, 2006).

Although this earlier work provides a general outline of changes in Jakobshavn Isbræ through the Holocene, chronological uncertainties make it difficult to assess the rates of past ice-margin changes. Also, the relationship between past ice-margin fluctuations and temperature changes is difficult to evaluate, given chronological uncertainties combined with the lack of a local Holocene temperature record. Here we combine 18 ^{10}Be surface exposure ages (herein ^{10}Be ages) spanning from the fjord mouth (Isfjeldsbanken) to just beyond the historic moraine (Weidick, 1968) with radiocarbon-dated lake sediments from a proglacial/threshold lake (e.g., Kaplan et al., 2002) to reconstruct, in more chronologic detail than previously available, Jakobshavn Isbræ fluctuations throughout the Holocene (Fig. 1; see the GSA Data Repository[1] for methods).

RESULTS

All ^{10}Be exposure ages were calculated using the CRONUS-Earth online exposure age calculator and a regionally calibrated North American ^{10}Be production rate (Balco et al., 2009; Tables DR1 and DR2 in the Data Repository). The ^{10}Be ages from sculpted bedrock surfaces (n = 14) and erratic boulders (n = 4) range from 12.0 ± 0.3 to 7.3 ± 0.3 ka. Five ^{10}Be ages located outboard of the Fjord Stade moraines (Fig. 1) record the timing of deglaciation of the fjord mouth at 10.2 ± 0.1 ka, consistent with the timing of deglaciation inferred from minimum constraining radiocarbon ages near the coast (Long et al., 2006; Weidick and Bennike, 2007; Table DR3). Following deglaciation of the outer Isfjord at 10.2 ka and deposition of the Marrait moraine some time thereafter, an advance of Jakobshavn Isbræ culminated with deposition of the Tasiussaq moraine slightly before 8.0 ± 0.2 ka (n = 5). Furthermore, we identified in the field a location north of the Isfjord where the Tasiussaq moraine overlaps the Marrait moraine, and the Tasiussaq moraine is the only moraine present near the fjord mouth. Thus, both the gap in time between initial deglaciation and Tasiussaq moraine deposition, and the crosscutting moraines suggest that this moraine represents an advance of Jakobshavn Isbræ . Radiocarbon ages from basal lacustrine sediments ~20 km upfjord from the fjord mouth indicate deglaciation of the middle Isfjord by ca. 7600 cal yr B.P. (Long et al., 2006; Fig. 1). Six ^{10}Be ages from bedrock immediately outboard of the Little Ice Age (LIA) moraine average 7.5 ± 0.2 ka, indicating the time when Jakobshavn Isbræ retreated behind this position.

To assess the history of Jakobshavn Isbræ after ice had retreated behind its LIA margin at 7.5 ± 0.2 ka, we collected sediment cores from Iceboom Lake (informal name; 69°14′17″N, 50°00′09″W; ~180 m above sea level, masl), located immediately outboard of the LIA moraine and 2 km north of Jakobshavn Isfjord (Fig. 1). Iceboom Lake currently does not receive meltwater from the GIS and is dominated by organic sedimentation (Fig. 2); however, during phases when the GIS was more extensive than today, but not overriding the lake, the GIS spilled silt-laden meltwater into the lake catchment. As a result, sediment cores (08ICE-3, 08ICE-5) collected from two subbasins within Iceboom Lake contain alternating units of minerogenic and organic-rich sediments (Fig. 2). We used radiocarbon ages on macrofossils to date the sharp contacts between these

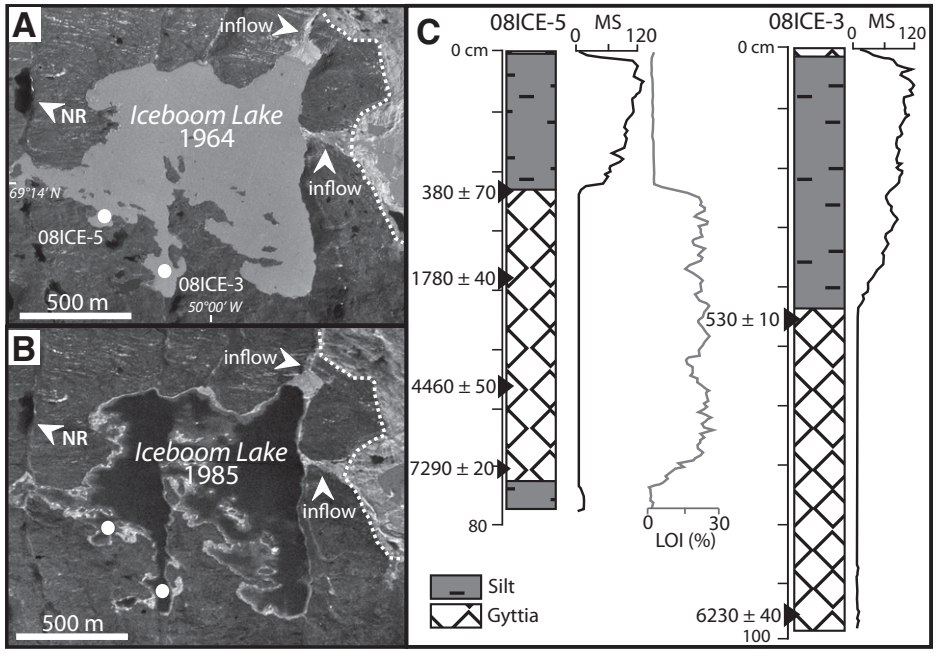

Figure 2. Results from Iceboom Lake (location shown in Fig. 1). A: 1964 aerial photo of Iceboom Lake receiving minerogenic input from Greenland Ice Sheet (GIS) meltwater. Little Ice Age margin (dashed line) and inflows (arrows) can be seen on right side of photo along with coring locations. NR—location of North Lake chironomid record. B: 1985 aerial photo of Iceboom Lake. Note color difference between photos, as Iceboom Lake was no longer receiving GIS meltwater in 1985. C: Stratigraphic logs of two cores from Iceboom Lake with ^{14}C ages (cal yr B.P.; 1 standard deviation). MS—magnetic susceptibility; LOI—loss on ignition.

[1]GSA Data Repository item 2011067, materials and methods, Figure DR1, Tables DR1–DR4, is available online at www.geosociety.org/pubs/ft2011.htm, or on request from editing@geosociety.org or Documents Secretary, GSA, P.O. Box 9140, Boulder, CO 80301, USA.

units (e.g., Kaplan et al., 2002). A radiocarbon age of 7290 ± 20 cal yr B.P. (Table DR4) from organic sediments slightly above basal minerogenic sediments in 08ICE-5 constrains the timing when the ice margin retreated out of the lake's catchment, and is consistent with ^{10}Be ages of 7.4 ± 0.4 and 7.4 ± 0.2 ka from bedrock near the lake (Fig. 3). Above the basal minerogenic unit are organic-rich sediments, which in turn are overlain by a unit of glacially derived, laminated minerogenic sediments. Radiocarbon ages from just below the upper minerogenic sediments in the two cores are 530 ± 10 and 380 ± 70 cal yr B.P. (Fig. 2). Radiocarbon ages from throughout the organic-rich unit indicate continuous organic sedimentation and no GIS meltwater input between 7300 and ca. 400 cal yr B.P. Following occupation of Iceboom Lake's catchment by the GIS during the LIA, the lake catchment became ice free some time between A.D. 1964 and 1985 (Fig. 2), when the current period of organic sedimentation began.

The response of Jakobshavn Isbræ to Holocene climate change can be evaluated by comparing this newly detailed picture of Holocene retreat and regrowth to independent records of regional temperature change. We present estimates of temperature change by using insect remains (Diptera: Chironomidae, i.e., chironomids) preserved in sediments from North Lake (informal name; 69°14′28″N, 50°01′41″W; ~180 masl; Fig. 2) to reconstruct local summer temperatures throughout the middle and late Holocene. Our reconstruction depicts summer temperatures that were 2 °C warmer than modern between ca. 6 and 4.5 cal kyr B.P., near-modern values by ca. 2.5 cal kyr B.P., and summer temperatures ~1 °C cooler than modern recorded in the uppermost sediments (Fig. 3; Fig. DR1).

DISCUSSION

Our most ice-distal ^{10}Be ages, combined with previously published ages from Disko Bugt, indicate the retreat of the Jakobshavn ice margin at least to the Isfjord mouth, and likely farther inland, at 10.2 ka. This phase of deglaciation coincided with a period of warmth inferred from paleoclimate reconstructions, which suggest rapidly rising mean annual temperatures in the early Holocene over central Greenland (e.g., Dahl-Jensen et al., 1998; Vinther et al., 2009), with summers as much as 5 °C warmer than today on nearby Baffin Island (Axford et al., 2009). Our ^{10}Be ages indicate that Jakobshavn Isbræ advanced slightly before 8.0 ± 0.2 ka, marked by deposition of the Tasiussaq moraine. The timing of this advance suggests it may have been related to the cold reversal ca. 8.2 ka (e.g., Alley et al., 1997; Long and Roberts, 2002), which would imply a rapid ice-margin response to a centennial-scale climate perturbation. However, other work has suggested that deposition of the Fjord Stade moraines across central-west Greenland occurred asynchronously (e.g., Long et al., 2006), and may not represent a clear response to the 8.2 ka event. Nonetheless, our chronology suggests that of the Fjord Stade moraines present at the Jakobshavn Isbræ fjord mouth, the Tasiussaq moraine was deposited in response to the 8.2 ka event.

Final deglaciation of the Isfjord commenced at 8 ka, with ~50 km of retreat occurring between 8.0 ± 0.2 ka and 7.5 ± 0.2 ka, yielding an average retreat rate of ~100 m yr^{-1}. ^{10}Be ages of 7.5 ± 0.2 and 7.3 ± 0.3 ka ~10–15 km north of the Isfjord (Fig. 1) indicate that deglaciation of the land-based margin north of the Isfjord was synchronous with deglaciation of the main Isfjord. This period of rapid retreat within and beyond the Isfjord was coincident with increasing regional temperatures inferred from boreholes at the Greenland Ice Core Project (GRIP) ice-core sites (Dahl-Jensen et al., 1998; Fig. 3). In addition, marine sediment cores in Disko Bugt show faunal assemblage changes ca. 7.8 cal kyr B.P. that imply an incursion of the warm West Greenland Current into eastern Disko Bugt (Lloyd et al., 2005). The influx of warm water may have partly contributed to increased melting of the glacier terminus, as has been proposed for latest twentieth century retreat (Holland et al., 2008). This period of warming likely forced ice-margin retreat from the shallow fjord mouth into deeper water, promoting increased calving rates and further retreat (Briner et al., 2009; Benn et al., 2007).

Sediments from Iceboom Lake and ^{10}Be ages both indicate that Jakobshavn Isbræ retreated behind its LIA margin, and considering Jakobshavn Isbræ's rapid rate of retreat, likely behind its current margin, ca. 7.5 ka. Although local and regional reconstructions of late Holocene cooling indicate that temperatures approached modern preindustrial values by ca. 2.5 ka (e.g., Dahl-Jensen et al., 1998; Kaplan et al., 2002), evidence from Iceboom Lake reveals that the ice did not advance to near its current position until ~2 k.y. later (i.e., the LIA; Fig. 3). This suggests that during the middle Holocene, when the chironomid record from North Lake indicates that summer temperatures near Jakobshavn were 2 °C warmer than modern, the ice margin was substantially more reduced than today (Weidick et al., 1990). By inferring that the geometry of the ice margin during its advance into Iceboom

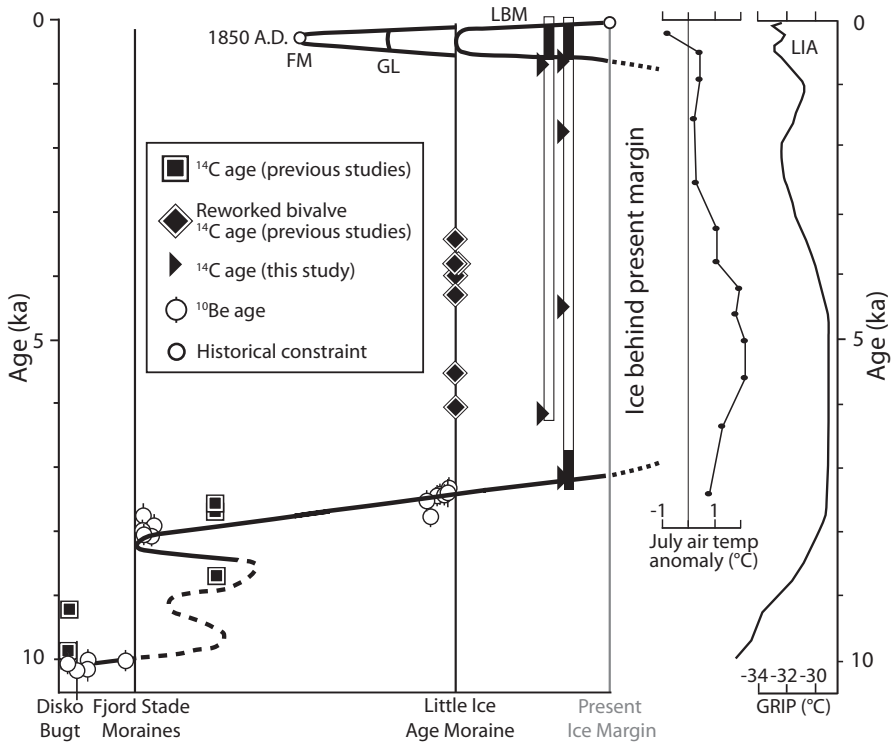

Figure 3. Time-distance diagram for Jakobshavn Isbræ. Compilation of ice-margin constraints at Jakobshavn Isbræ plotted versus relative distance. Outer Isfjord deglaciated at 10.2 ± 0.1 ka followed by deglaciation from younger Fjord Stade moraine (Tasiussaq) at 8.0 ± 0.2 ka. Ice had retreated behind Little Ice Age (LIA) margin by 7.5 ± 0.2 ka, where it remained until ca. A.D. 1500–1640, when the Jakobshavn Isbræ floating margin (FM), grounding line (GL), and land-based margin (LBM) advanced. Ice-margin fluctuations are compared with local summer temperatures anomalies inferred from local chironomids and borehole-inferred temperatures over Greenland (Dahl-Jensen et al., 1998). Detailed radiocarbon information is provided in Table DR3 (see footnote 1). GRIP—Greenland Ice Core Project.

Lake's catchment was similar to when the ice margin retreated out of the catchment, we suggest that beginning some time between A.D. 1500 and 1640 and continuing through A.D. 1850, the Jakobshavn Isbræ grounding line advanced at least 15 km through the Isfjord (measured from LIA grounding line to 2008 grounding line), and the adjacent land-based margin advanced ~2–4 km. Historical observations indicate that the ice margin remained at its LIA maximum position until A.D. 1850 (Weidick and Bennike, 2007). The current period of retreat began ca. A.D. 1850–1900, coinciding with an ~2 °C (~0.5 °C) increase in mean annual (July) temperature from 1873 to 2001, measured near Jakobshavn (Box, 2002).

CONCLUSIONS

Ice-margin advance during the early Holocene, likely driven by one or more abrupt climate reversals, combined with ice-margin changes during and after the LIA suggest that Jakobshavn Isbræ responds rapidly to centennial-scale climate perturbations. Cooling during the LIA (~1 °C) resulted in ~15 and 25 km of advance of Jakobshavn Isbræ's grounding line and floating terminus through the Isfjord, respectively; similarly, tens of kilometers of retreat were driven by relatively modest changes in atmospheric and ocean temperatures since A.D. 1850. Within centuries after ice withdrew from the fjord mouth in the early Holocene, Jakobshavn Isbræ retreated to behind its current margin, where it remained for ~7 k.y. in response to sustained warmer-than-present temperatures (~2 °C) during the middle Holocene (Fig. 3). In summary, the Jakobshavn marine terminus has demonstrated sensitivity to decadal- to millennial-scale Holocene temperature trends. Although the adjacent land-based margin underwent more moderate LIA advance and subsequent retreat since A.D. 1850, the land-based margin retreated at a rate similar to that of Jakobshavn Isbræ earlier in the Holocene. Thus, geological data suggest that both marine- and land-terminating margins of the western GIS will likely undergo significant and prolonged retreat if future temperatures match those reached during the middle Holocene.

ACKNOWLEDGMENTS

We thank CH2M Hill for logistical support, W. Phillips and S. McGrane, who aided in collecting and processing ^{10}Be samples, and O. Darko and S. Truex, who aided in lake sediment analysis. We also thank I. Walker and D. Francis for sharing chironomid training set data, E. Thomas for discussions throughout the project duration, and three anonymous reviewers whose comments helped improve this manuscript. This work is supported by the Geography and Spatial Science Division of the U.S. National Science Foundation (NSF-BCS-0752848).

REFERENCES CITED

Alley, R.B., Mayewski, P.A., Sowers, T., Stuiver, M., Taylor, K.C., and Clark, P.U., 1997, Holocene climatic instability: A prominent, widespread event 8200 yr ago: Geology, v. 25, p. 483–486, doi:10.1130/0091-7613(1997)025<0483:HCIAPW>2.3.CO;2.

Alley, R.B., Clark, P.U., Huybrechts, P., and Joughin, I., 2005, Ice-sheet and sea-level changes: Science, v. 310, p. 456–460, doi:10.1126/science.1114613.

Axford, Y., Briner, J.P., Miller, G.H., and Francis, D.R., 2009, Paleoecological evidence for abrupt cold reversals during peak Holocene warmth on Baffin Island, Arctic Canada: Quaternary Research, v. 71, p. 142–149, doi:10.1016/j.yqres.2008.09.006.

Balco, G., Briner, J., Finkel, R.C., Rayburn, J.A., Ridge, J.C., and Schaefer, J.M., 2009, Regional beryllium-10 production rate calibration for northeastern North America: Quaternary Geochronology, v. 4, p. 93–107, doi:10.1016/j.quageo.2008.09.001.

Benn, D.I., Warren, C.R., and Mottram, R.H., 2007, Calving processes and the dynamics of calving glaciers: Earth-Science Reviews, v. 82, p. 143–179, doi:10.1016/j.earscirev.2007.02.002.

Box, J.E., 2002, Survey of Greenland instrumental temperature records: 1873–2001: International Journal of Climatology, v. 22, p. 1829–1847, doi:10.1002/joc.852.

Briner, J.P., Bini, A.C., and Anderson, R.C., 2009, Rapid early Holocene retreat of a Laurentide outlet glacier through an Arctic fjord: Nature Geoscience, v. 2, p. 496–499, doi:10.1038/ngeo556.

Clarke, T.S., and Echelmeyer, K., 1996, Seismic-reflection evidence for a deep subglacial trough beneath Jakobshavn Isbræ, West Greenland: Journal of Glaciology, v. 42, p. 219–232.

Csatho, B., Schenk, T., van der Veen, C.J., and Krabill, W.B., 2008, Intermittent thinning of Jakobshavn Isbræ, west Greenland, since the Little Ice Age: Journal of Glaciology, v. 54, p. 131–144, doi:10.3189/002214308784409035.

Dahl-Jensen, D., Mosegaard, K., Gundestrup, N., Clow, G.D., Johnsen, S.J., Hansen, A.W., and Balling, N., 1998, Past temperatures directly from the Greenland Ice Sheet: Science, v. 282, p. 268–271, doi:10.1126/science.282.5387.268.

Holland, D.M., Thomas, R.H., Young, B.D., Ribergaard, M.H., and Lyberth, B., 2008, Acceleration of Jakobshavn Isbræ triggered by warm subsurface ocean waters: Nature Geoscience, v. 1, p. 659–664, doi:10.1038/ngeo316.

Joughin, I., Abdalati, W., and Fahnestock, M., 2004, Large fluctuations in speed on Greenland's Jakobshavn Isbrae glacier: Nature, v. 432, p. 608–610, doi:10.1038/nature03130.

Kaplan, M.R., Wolfe, A.P., and Miller, G.H., 2002, Holocene environmental variability in southern Greenland inferred from lake sediments: Quaternary Research, v. 58, p. 149–159, doi:10.1006/qres.2002.2352.

Kaufman, D.S., and 29 others, 2004, Holocene thermal maximum in the western Arctic (0–180°W): Quaternary Science Reviews, v. 23, p. 529–560, doi:10.1016/j.quascirev.2003.09.007.

Lloyd, J.M., 2006, Late Holocene environmental change in Disko Bugt, west Greenland: Interaction between climate, ocean circulation and Jakobshavn Isbrae: Boreas, v. 35, p. 35–49, doi:10.1080/03009480500359061.

Lloyd, J.M., Park, L.A., Kuijpers, A., and Moros, M., 2005, Early Holocene paleoceanography and deglacial chronology of Disko Bugt, west Greenland: Quaternary Science Reviews, v. 24, p. 1741–1755, doi:10.1016/j.quascirev.2004.07.024.

Long, A.J., 2009, Back to the future: Greenland's contribution to sea-level change: GSA Today, v. 19, p. 4–10, doi:10.1130/GSATG40A.1.

Long, A.J., and Roberts, D.H., 2002, A revised chronology for the 'Fjord Stade' moraine in Disko Bugt, west Greenland: Journal of Quaternary Science, v. 17, p. 561–579, doi:10.1002/jqs.705.

Long, A.J., and Roberts, D.H., 2003, Late Weichselian deglacial history of Disko Bugt, West Greenland, and the dynamics of the Jakobshavn Isbræ ice stream: Boreas, v. 32, p. 208–226, doi:10.1080/03009480310001119.

Long, A.J., Roberts, D.H., and Dawson, S., 2006, Early Holocene history of the west Greenland Ice Sheet and the GH-8.2 event: Quaternary Science Reviews, v. 25, p. 904–922, doi:10.1016/j.quascirev.2005.07.002.

Pfeffer, W.T., Harper, J.T., and O'Neel, S., 2008, Kinematic constraints on glacier contributions to 21st-century sea-level rise: Science, v. 321, p. 1340–1343, doi:10.1126/science.1159099.

Pritchard, H.D., Arthern, R.J., Vaughn, D.G., and Edwards, L.A., 2009, Extensive dynamic thinning on the margins of the Greenland and Antarctic ice sheets: Nature, v. 461, p. 971–975, doi:10.1038/nature08471.

Rignot, E., and Kanagaratnam, P., 2006, Changes in the velocity structure of the Greenland Ice Sheet: Science, v. 311, p. 986–990, doi:10.1126/science.1121381.

Simpson, M.J.R., Milne, G.A., Huybrechts, P., and Long, A.J., 2009, Calibrating a glaciological model of the Greenland Ice Sheet from the Last Glacial Maximum to present-day using field observations of relative sea level and ice extent: Quaternary Science Reviews, v. 28, p. 1631–1657, doi:10.1016/j.quascirev.2009.03.004.

van den Brooke, M., Bamber, J., Ettema, J., Rignot, E., Schrama, E., van de Berg, W.J., van Meijgard, E., Velicogna, I., and Wouters, B., 2009, Partitioning recent Greenland mass loss: Science, v. 326, p. 984–986, doi:10.1126/science.1178176.

Vinther, B.L., and 13 others, 2009, Holocene thinning of the Greenland ice sheet: Nature, v. 461, p. 385–388, doi:10.1038/nature08355.

Weidick, A., 1968, Observations on some Holocene glacier fluctuations in west Greenland: Meddelelsser om Grønland 165, 202 p.

Weidick, A., and Bennike, O., 2007, Quaternary glaciation history and glaciology of Jakobshavn Isbræ and the Disko Bugt region, West Greenland: A review: Geological Survey of Denmark and Greenland Bulletin 14, 78 p.

Weidick, A., Oerter, H., Reeh, N., Thomsen, H.H., and Thorning, L., 1990, The recession of the inland ice margin during the Holocene Climatic Optimum in the Jakobshavn-Isfjord area of West Greenland: Global and Planetary Change, v. 82, p. 389–399, doi:10.1016/0921-8181(90)90010-A.

Manuscript received 19 May 2010
Revised manuscript received 2 September 2010
Manuscript accepted 9 September 2010

Printed in USA

Response of Jakobshavn Isbræ, Greenland, to Holocene climate change

Nicolás E. Young, Jason P. Briner, Heather A.M. Stewart, Yarrow Axford, Beata Csatho, Dylan H. Rood, and Robert C. Finkel

^{10}Be dating

Samples from sculpted gneiss bedrock surfaces (n = 14) and perched erratics (n = 4) were collected with a hammer and chisel. Samples were collected from horizontal to near-horizontal surfaces and we avoided sampling from boulder edges and corners. Geographic coordinates and elevation for each sample were collected with a handheld GPS device, and a clinometer was used to measure shielding by surrounding topography for two samples (FST08-BR; FST08-04). Remaining samples did not require measurement of the surrounding topography. Samples were collected at elevations above the local marine limit, which is at least 80 m.a.s.l. near the outer coast and ~40 m.a.s.l. inboard of the Fjord Stade moraines (Long et al., 2006, Long and Roberts, 2002). Fjord Stade moraines adjacent to the Isfjord shown in figure 1 (main text) were initially mapped on aerial photographs and then checked in the field by walking their respective crests with a handheld GPS unit.

All samples were processed at the University at Buffalo Cosmogenic Isotope Laboratory following procedures modified from Kohl and Nishiizumi (1992). Samples were first crushed and sieved to isolate the 425-850 μm size fraction and then pretreated in dilute HCl and HNO_3-HF acid baths. Quartz was isolated by heavy-liquid mineral separation and additional HNO_3-HF heated sonification baths. ^{9}Be carrier (~0.25-0.45 mg) was added to each sample prior to dissolution in concentrated HF. Beryllium was extracted using ion-exchange chromatography, selective precipitation with NH_4OH, and final oxidation to BeO.

^{10}Be/^{9}Be AMS measurements were completed at the Lawrence Livermore National Laboratory Center for Mass Spectrometry and normalized to standard 07KNSTD3110 (Nushiizumi et al., 2007). Ratios for dissolution process blanks (n = 3) averaged 2.10×10^{-14} with a lowest achieved process blank ratio of 2.10×10^{-15}. AMS precision for blank-corrected ^{10}Be/^{9}Be sample ratios ranged from 2.5-5.3%.

^{10}Be exposure ages (tables DR1, DR2) were calculated using the CRONUS-Earth online exposure age calculator (http://hess.ess.washington.edu/math; Version 2.2; Balco et al., 2008). As this region has undergone isostatic uplift since deglaciation, the measured sample elevation does not reflect the sample elevation history. Prior to calculating ^{10}Be exposure ages, sample elevation was corrected by using a minimum marine limit of 80 m asl, and a regional emergence curve spanning the last ~9.5 cal ka BP Long et al., 2006; Long and Roberts, 2002). We used isolation basin data from Long et al. (2006) and Long and Roberts (2002) to generate three separate emergence curves representing 1) emergence since ~9.5 cal ka BP for our most distal samples, 2) emergence since ~7.9 ka for samples located immediately inboard of the Tasiussaq moraine, and 3) emergence since ~7.4 cal ka BP for samples located just outboard of the LIA margin. Emergence data was plotted graphically, fit with a 3rd order polynomial trend line, and finally the trend line for each equation was solved. Emergence curve

solutions provide the necessary elevation corrections needed for each sample. Resulting elevation corrections are -15.6 m for samples located outboard of the Fjord Stade (FS) moraines, -4.6 m for samples located immediately inboard of the FS moraines, and -0.2 m for samples located just beyond the LIA margin. We employed a regionally calibrated ^{10}Be production rate of 3.93±0.19 atoms g^{-1} yr^{-1} (i.e. Balco et al., 2009) and the constant-production scaling scheme of Lal/Stone (Lal, 1991; Stone, 2000), resulting in ^{10}Be exposure ages ~12% older than ages calculated using the globally-calibrated production rate of 4.49±0.43 atoms g^{-1} yr^{-1} (Balco et al., 2008). These values are lower than the production rates reported in Balco et al. (2008) and Balco et al. (2009) and reflect a recent update to the Be isotope ratio standard of Nishiizumi et al. (2007; 07KNSTD3110). Full documentation of this change is available at the aforementioned CRONUS-Earth website. As the influence of the earth's magnetic field on ^{10}Be production is negligible at the study area's relatively high latitude (~69ºN; Gosse and Phillips, 2001), all ^{10}Be exposure ages reported in the main text use the constant-production scheme of Lal/Stone (1991; 2000; table DR1). ^{10}Be ages using alternative scaling schemes (i.e. Lifton et al., 2005; Desilets and Zreda, 2003; Desilets et al., 2006; Dunai, 2001) that incorporate time-dependent production rates based on fluctuations in the earth's magnetic field are presented in table DR2. ^{10}Be ages calculated using these scaling schemes result in age differences that are minimal (<2%), and while different scaling schemes may alter absolute ^{10}Be ages, our relative chronology remains unchanged.

Both snow cover and erosion can lead to apparent ^{10}Be exposure ages that are younger than absolute ^{10}Be ages. Bedrock samples were collected from windswept locations (i.e. ridge crests) and all sampled boulders were at least 2.5 m tall. We observe no correlation between boulder height and ^{10}Be age, which would be expected with significant snow cover. We consider the effects of snow cover minimal and note that glacial polish and striations were routinely observed on both bedrock and boulder surfaces, indicating negligible erosion. Thus, presented ^{10}Be ages are not corrected for shielding by snow cover or erosion.

Sample FST08-BR, which yielded a ^{10}Be age of 12.0±0.3 ka was not included in our discussion and likely contains ^{10}Be inherited from a previous period of exposure. This sample is >2σ older than all remaining samples located just inside of the FS moraines and FST08-04, which was collected immediately adjacent to FST08-BR, has a ^{10}Be age of 8.1±0.3 ka. Moreover, sample FST08-BR is >2σ older than samples located outside of the FS moraines (10.2±0.1 ka; n = 5).

Lake sediment cores

Multiple sediment cores for this study were collected from two lakes (Fig. 2). Lake bathymetry was determined using a Garmin GPSMAP 400 series GPS receiver connected to a dual beam depth transducer. Sediment cores were collected using the Universal Coring system (Aquatic Research Instruments; www.aquaticresearch.com) with 5-cm-diameter polycarbonate core tubes; sediment cores were recovered with intact sediment-water interfaces, which were allowed to dewater for several days prior to being packaged for transport to the University at Buffalo. In the lab, cores were split

lengthwise, photographed and logged. Magnetic susceptibility (MS) was measured every 0.5 cm using a Bartington MS2E High Resolution Surface Scanning Sensor scanner connected to a Bartington MS2 Magnetic Susceptibility Meter. Organic matter content was measured every 0.5 cm using the loss-on-ignition (LOI) procedure at 550°C. Multiple sediment cores were obtained from Iceboom lake, which has a complex bathymetry and several different sub-basins; cores were collected from the deepest point in two sub-basins on the opposite side of the lake from the inflow sources. 08ICE-3 is 99 cm long and was collected at 12.21 m depth (69°13'58" N, 50°35'00" W); 08ICE-5 is 76 cm long and was collected at 3.12 m water depth (69°14'8" N, 50°1'7" W). The general stratigraphy, MS and LOI data are shown in figure 2. A sediment core was also collected from small lake 300 m north of Iceboom Lake's outflow that has not been connected to the ice sheet drainage network since deglaciation. 08NOR-3 is 106 cm long and was collected at 3.85 m water depth (69°14'29.82"N, 50° 1'38.01"W). The bottom 2 cm in the core comprise organic-poor sand, which is overlain by organic rich lake sediment.

Pieces of aquatic moss were picked for ^{14}C dating from two intervals in 08ICE-3, four intervals in 08ICE-5, and three intervals in 08NOR-3 (Table DR4). After being washed with deionized water at the University at Buffalo, cleaned samples were subsequently prepared at the INSTAAR Laboratory for AMS Radiocarbon Preparation and Research at the University of Colorado and measured at the W.M. Keck Carbon Cycle AMS Facility at the University of California, Irvine. Radiocarbon ages were calibrated with CALIB v 6.0 (http://radiocarbon.pa.qub.acuk/calib/; Stuiver et al., 2010) and the IntCal09 calibration curve (Reimer et al., 2009).

The basal radiocarbon age from 08ICE-5 and the ^{10}Be ages for deglaciation match well. However, the basal radiocarbon age from 08NOR-3 is ~500 yr older than both the basal radiocarbon age from 08ICE-5 and the ^{10}Be ages for deglaciation near the Neoglacial maximum ice margin. Additionally, the $\delta^{13}C$ value of the macrofossils that were dated is atypical of all other macrofossils dated from lakes in this region, implying a complicated carbon pool in the lake. Furthermore, a marine influence on the $\delta^{13}C$ value is highly unlikely as North Lake rests at ~180 m.a.s.l., well above the local marine limit (~40 m.a.s.l.). In any case, because the majority of the geochronology suggests deglaciation of NOR and ICE lakes occurred ~7.4 ka, we use 7400 cal yr BP for the initiation of organic matter deposition in 08NOR-3. Our temperature reconstruction presented in figure 3 (main text) depicts the onset of organic sedimentation at 7.4 ka.

Chironomids

Chironomids (non-biting midges, Diptera: Chironomidae) were analyzed at 13 depths in the 08NOR-3 sediment core (Figs. 3, DR1) and in a surface sediment sample collected from the same lake in 2009. Sediment samples were deflocculated with warm 5% KOH for 20 minutes and rinsed on a 100μm mesh sieve. Head capsules were manually picked from a Bogorov sorting tray under a 40x power dissecting microscope, then permanently mounted on slides using Euparal. All samples contained at least 50 whole identifiable head capsules, and 11 different fossil taxa were enumerated. Chironomids were analyzed according to standard protocol (e.g. Walker, 2001) and taxonomic identifications followed Brooks et al. (2007) with reference to Oliver and

Roussel (1983) and Wiederholm (1983), and taxa were lumped to harmonize with Francis et al. (2006).

July air temperatures were modeled using a chironomid-temperature transfer function developed for northeastern North America, which includes training set (calibration) sites in the Eastern Canadian Arctic west of Greenland (Francis et al., 2006; Walker et al., 1997). The weighted-averaging regression model uses square-root transformed species data and has a root mean squared error of prediction (RMSEP) of 1.5°C for mean July air temperatures. This transfer function has previously been used to reconstruct Holocene paleotemperatures at a lake in west Greenland (e.g. Wooller et al., 2004), as well as numerous lakes in the Canadian Arctic (Axford et al., 2009; Francis et al., 2006; Briner et al., 2006). Paleotemperatures were modeled using the software program C2 v 1.4.3 (Juggins, 2003), and are expressed as anomalies (in °C) relative to the modern estimate from North Lake surface sediments (Figs. 3, DR1). The applicability of the transfer function to the fossil data was assessed by two means: One, it was noted that all fossil taxa were represented in the training set (*Tanytarsus lugens* type and *Micropsectra* type are lumped within Tanytarsini undiff. for the temperature modeling); and two, the statistical software package R v 2.2.1 was used to calculate the squared-chord distance (SCD) between each downcore assemblage and its closest analog in the training set. For all but one sample, SCD <0.5; the remaining sample has SCD 0.74 from its closest analog in the training set (Fig. DR1).

Supplemental References:

Balco, G., Stone, J.O., Lifton, N.A., and Dunai, T.J., 2008, A complete and easily accessible means of calculating surface exposure ages or erosion rates from ^{10}Be and ^{26}Al measurements: Quateranry Geochronology, v. 3, p. 174-195.

Balco, G., Briner, J., Finkel, R.C., Rayburn, J.A., Ridge, J.C., and Schaefer, J.M., 2009, Regional beryllium-10 production rate calibration for northeastern North America: Quaternary Geochronology, v. 4, p. 93-107.

Briner, J.P., Michelutti, N., Francis, D.R., Miller, G.H., Axford, Y., Woller, M.J., and Wolfe, A.P., 2006, A multi-proxy lacustrine record of Holocene climate change on northeastern Baffin Island, Arctic Canada: Quaternary Research, v. 65, 431-442.

Brooks, S.J., Langdon, P.G. and Heiri, O., 2007, The identification and use of Palaearctic Chironomidae larvae in palaeoecology. QRA Technical Guide 10, Quaternary Research Association, London. 276 p.

Desilets, D., and Zreda, M., 2003, Spatial and temporal distribution of secondary cosmic ray nucleon intensities and applications to in-situ cosmogenic dating: Earth and Planetary Science Letters, v. 206, p. 21–42.

Desilets, D., Zreda, M., and Prabu, T., 2006, Extended scaling factors for in situ cosmogenic nuclides: New measurements at low latitude: Earth and Planetary Science Letters, v. 246, p. 265-276.

Dunai, T.J., 2001, Influence of secular variation of the magnetic field on production rates of in situ produced cosmogenic nuclides: Earth and Planetary Science Letters, v. 193, p. 197-212.

Francis, D.R., Wolfe, A.P., Walker, I.R., and Miller, G.H., 2006, Interglacial and Holocene temperature reconstructions based on midge remains in sediments of two lakes from Baffin Island, Nunavut, Arctic Canada: Palaeogeography, Palaeoclimatology, Palaeoecology, v. 236, p. 107–124.

Gosse, J.C., and Phillips, F.M., 2001, Terrestrial in situ cosmogenic nuclides: theory and application: Quaternary Science Reviews, v. 20, p. 1475–1560.

Juggins, S., 2003, C2 User guide. Software for ecological and palaeoecological data analysis and visualization. University of Newcastle, Newcastle upon Tyne, UK. 69 p.

Kohl, C.P. and Nishiizumi, K., 1992. Chemical isolation of quartz for measurement of in situ- produced cosmogenic nuclides: Geochimica Cosmochimica Acta, v. 56, p. 3583–3587.

Lal, D., 1991, Cosmic ray labeling of erosion surfaces: *in situ* nuclide production rates and erosion models: Earth and Planetary Science Letters, v. 104, p. 424-439.

Lifton, N.A., Beiber, J.W., Clem, J.M., Duldig, M.L., Evenson, P., Humble, J.E., and Pyle, R., 2005, Addressing solar modulation and long-term uncertainties in scaling secondary cosmic rays for in situ cosmogenic nuclide applications: Earth and Planetary Science Letters, v. 239, p. 140-161.

Long, A.J., Roberts, D.H., and Dawson, S., 2006, Early Holocene history of the west Greenland Ice Sheet and the GH-8.2 event: Quaternary Science Reviews, v. 25, p. 904-922.

Nishiizumi, K., Imamura, M., Caffee, M., Southon, J., Finkel, R., and McAnich, J., 2007, Absolute calibration of 10Be AMS standards: Nuclear Instruments and Methods in Physics Research B, v. 258, p. 403-413.

Oliver, D.R., and Roussel, M.E., 1983, The Insects and Arachnids of Canada: Part 11. The Genera of Midges of Canada; Diptera: Chironomidae 1746, Agriculture Canada, Ottawa.

Reimer, P.J., Baillie, M.G.L., Bard, E., Bayliss, A., Beck, J.W., Blackwell, P.G., Bronk Ramsey, C., Buck, C.E., Burr, G.S., Edwards, R.L., Friedrich, M., Grootes, P.M., Guilderson, T.M., Hajdas, I., Heaton, T.J., Hogg, A.G., Hughen, K.A., Kaiser, K.F., Kromer, B., McCormac, F.G., Manning, S.W., Reimer, R.W., Richards, D.A., Southon, J.R., Talamo, S., Turney, C.S.M., van der plicht, J., and Weyhenmeyer, C.E., 2009, IntCal09 and Marine09 Radiocarbon Age Calibration Curves, 0–50,000 Years cal BP: Radiocarbon, v. 51, p. 1111-1150.

Stone, J.O., 2000, Air pressure and cosmogenic isotope production: Journal of Geophysical Research, v. 105, p. 23753–23759.

Stuiver, M., Reimer, P. J. and Reimer, R. W., 2010, CALIB 6.0. WWW program and documentation. Available at http://calib.qub.ac.uk/calib/.

Walker, I.R., in Tracking Environmental Change Using Lake Sediments, eds Smol, J.P., Birks, H.J.B., and Last, W.M., 2001, Kluwer, Dordrecht, The Netherlands) 4, 43-66.

Walker, I.R., Levesque, J., Cwynar, L.C. and Lotter, A.F., 1997, An expanded surface-water paleotemperature inference model for use with fossil midges from eastern Canada: Journal of Paleolimnology, v. 18, p. 165-178.

Weidick, A., 1972, C^{14} dating of survey material performed in 1971: Rapport Grønlands Geologiske Undersøgelse. v. 45, p. 58-67.

Weidick, A., and Bennike, O., 2007, Quaternary glaciation history and glaciology of Jakobshavn Isbræ and the Disko Bugt region, West Greenland: a review: Geological Survey of Denmark and Greenland Bulletin 14, 78 p.

Wiederholm, T. (Ed.), 1983, Chironomidae of the Holarctic Region. Keys and Diagnoses: Part 1. Larvae. Entomoogical Scandinivica Supplement 19, pp. 457.

Wooller, M.J., Franics, D., Fogel, M.L., Miller, G.F., Walker, I.R., Wolfe, A.P., 2004, Quantitative paleotemperature estimates from d18O of chironomid head capsules preserved in arctic lake sediments: Journal of Paleolimnology v, 31, p. 267-274.

Table DR1: ^{10}Be sample information for Jakobshavn Isbræ

Sample	Latitude (N)	Longitude (W)	Elevation (m asl)	Corrected elevation (m asl)[a]	Sample height (m)	Thickness (cm)	Shielding correction	Quartz (g)	Be carrier added (g)[b]	^{10}Be (atoms g^{-1})	^{10}Be uncertainty (atoms g^{-1})	^{10}Be age[c]
Outboard of Fjord Stade moraines												
JAKN08-01	69° 12.331'	51° 07.465'	112	96	0	2.5	1.000	80.0463	0.4480	47575.8166	1168.264	10.2 ± 0.2
JAKN08-08	69° 11.958'	50° 58.043'	338	322	0	1.0	1.000	85.0596	0.2969	61424.170	1727.041	10.3 ± 0.3
JAKN08-21	69° 14.594'	50° 58.842'	390	374	0	1.0	1.000	75.4874	0.3800	63882.262	3382.958	10.2 ± 0.5
JAKN08-22	69° 14.459'	50° 57.683'	360	344	3.0	4.5	1.000	80.1615	0.3930	59644.6241	1868.383	10.1 ± 0.3
09GRO-01	69° 06.590'	51° 02.487'	204	188	0	5.0	1.000	77.0936	0.2514	50245.693	1253.572	10.0 ± 0.2
Inboard of Fjord Stade moraines												
JAKN08-13	69° 11.065'	50° 54.359'	180	175	0	2.5	1.000	80.1692	0.4570	41081.8675	1042.701	8.1 ± 0.2
FST08-BR	69° 11.844'	51° 03.244'	65	60	0	2.0	0.999	80.0250	0.2513	53768.095	1337.201	12.0 ± 0.3
FST08-04	69° 08.792'	51° 03.225'	65	60	2.5	2.0	0.999	80.3201	0.2511	36283.838	940.838	8.1 ± 0.2
09GRO-03	69° 06.820'	51° 03.858'	124	119	0	3.0	1.000	76.7977	0.2512	38918.931	1139.028	8.1 ± 0.2
09GRO-06	69° 06.970'	50° 59.467'	245	240	2.5	4.5	1.000	74.5675	0.2515	41475.243	1323.184	7.8 ± 0.2
09GRO-33	69° 11.469'	51° 00.441'	125	120	2.5	4.5	1.000	76.0270	0.2517	37484.239	1168.586	8.0 ± 0.2
Little Ice Age margin												
JAKN08-28	69° 14.444'	49° 59.109'	215	215	0	1.0	1.000	85.0930	0.3015	39588.0588	1902.308	7.4 ± 0.4
JAKN08-39	69° 13.283'	49° 59.712'	206	206	0	3.0	1.000	85.3685	0.2988	38695.1865	1261.777	7.4 ± 0.2
JAKN08-40	69° 13.536'	50° 03.411'	147	147	0	2.0	1.000	80.0340	0.4563	38904.9208	996.522	7.9 ± 0.2
JAKN08-44	69° 18.465'	50° 08.873'	347	347	0	2.0	1.000	80.2219	0.4103	44534.0809	1675.958	7.3 ± 0.3
JAKN08-56	69° 18.030'	50° 19.723'	425	425	0	1.0	1.000	80.0070	0.4539	49360.0035	1214.232	7.5 ± 0.2
JAKS08-33	69° 08.823'	50° 07.471'	222	222	0	1.0	1.000	80.2910	0.4062	40672.5553	1726.658	7.5 ± 0.3
JAKS08-34	69° 08.792'	50° 06.220'	180	180	0	2.0	1.000	80.1042	0.4540	38012.879	975.175	7.4 ± 0.2

[a]Sample elevation was corrected using a regional emergence curve with a marine limit of 80 m asl; elevations have been rounded to the nearest m

[b]All samples were spiked with a 405µg/g ^{9}Be carrier and AMS results are standardized to 07KNSTD3110

[c]Be ages given in ka at 1SD using the scaling scheme of Lal (1991)/Stone (2000). Comparison with other scaling schemes are shown in Table S2

Table DR2: ^{10}Be ages using alternative scaling schemes

Sample	St	De	Du	Li	Lm
Outboard of Fjord Stade moraines					
JAKN08-01	10.2 ± 0.2	10.0 ± 0.2	9.9 ± 0.2	9.8 ± 0.2	10.4 ± 0.2
JAKN08-08	10.3 ± 0.3	10.3 ± 0.3	10.1 ± 0.3	10.1 ± 0.3	10.5 ± 0.3
JAKN08-21	10.2 ± 0.5	10.2 ± 0.5	10.0 ± 0.5	9.9 ± 0.5	10.3 ± 0.5
JAKN08-22	10.1 ± 0.3	10.1 ± 0.3	9.9 ± 0.3	9.8 ± 0.3	10.2 ± 0.3
09GRO-01	10.0 ± 0.2	9.9 ± 0.2	9.7 ± 0.2	9.7 ± 0.2	10.1 ± 0.2
Inboard of Fjord Stade moraines					
JAKN08-13	8.1 ± 0.2	8.0 ± 0.2	7.9 ± 0.2	7.8 ± 0.2	8.2 ± 0.2
FST08-BR	12.0 ± 0.3	11.7 ± 0.3	11.5 ± 0.3	11.5 ± 0.3	12.1 ± 0.3
FST08-04	8.1 ± 0.2	7.9 ± 0.2	7.7 ± 0.2	7.7 ± 0.2	8.2 ± 0.2
09GRO-03	8.1 ± 0.2	8.0 ± 0.2	7.9 ± 0.2	7.9 ± 0.2	8.3 ± 0.2
09GRO-06	7.8 ± 0.2	7.7 ± 0.2	7.6 ± 0.2	7.5 ± 0.2	7.9 ± 0.2
09GRO-33	8.0 ± 0.2	7.8 ± 0.2	7.7 ± 0.2	7.6 ± 0.2	8.1 ± 0.2
Little Ice Age margin					
JAKN08-28	7.4 ± 0.4	7.3 ± 0.2	7.2 ± 0.2	7.2 ± 0.2	7.5 ± 0.2
JAKN08-39	7.4 ± 0.2	7.4 ± 0.3	7.2 ± 0.3	7.2 ± 0.3	7.5 ± 0.3
JAKN08-40	7.9 ± 0.2	7.8 ± 0.2	7.7 ± 0.2	7.6 ± 0.2	8.0 ± 0.2
JAKN08-44	7.3 ± 0.3	7.3 ± 0.2	7.2 ± 0.2	7.2 ± 0.2	7.5 ± 0.2
JAKN08-56	7.5 ± 0.2	7.5 ± 0.2	7.4 ± 0.2	7.3 ± 0.2	7.6 ± 0.2
JAKS08-33	7.5 ± 0.3	7.5 ± 0.3	7.4 ± 0.3	7.3 ± 0.3	7.7 ± 0.3
JAKS08-34	7.4 ± 0.2	7.3 ± 0.2	7.2 ± 0.2	7.2 ± 0.2	7.5 ± 0.2

^{10}Be exposure ages calcuated using a regionally calibrated North American production rate (Balco et al., 2009) and five scaling schemes: *St,* (Lal, 1991, and Stone 2000) from table DR1; *De* (Desilets and others, 2003, 2006); *Du* (Dunai, 2001); *Li* (Lifton et al., 2005); and *Lm* (Lal, 1991 and Stone 2000 - time dependent)

Table DR3: Preexisting radiocarbon information

Latitude N	Longtitude W	Material Dated	Radiocarbon Age (^{14}C yr BP)	Calibrated Age (cal yr BP ± 2σ)	δ^{13}C (‰PDB)	Lab Number	Reference
Deglaciation of Isfjord							
69º12′	51º04′	*Macoma calcarea* shell	8795±130	9470±350[a]	0	Ua-1086	Weidick and Bennike, 2007
69º06′	51º04′	shells	8630±130	9787±366	NA	K-1818	Weidick, 1972
69º07′	50º37′	bulk sediment	6750±40	7599±75	-21.4	Beta-178169	Long et al., 2006
68º07′	50º35′	bulk sediment	6910±40	7767±96	-20.5	Beta-178170	Long et al., 2006
69º07′	50º38′	bulk sediment	7960±40	8819±172	-20.7	Beta-178168	Long et al., 2006
Reworked marine fauna in historic moraine							
68º06′	50º02′	*Mya truncata* shell	3590±65	3492±156[a]	1.88	Ua-4581	Weidick and Bennike, 2007
68º06′	50º02′	*Hiatella artica* shell	3940±65	3935±190[a]	1.92	Ua-4582	Weidick and Bennike, 2007
68º06′	50º02′	*Mya truncata* shell	3945±70	3933±204[a]	2.50	Ua-4580	Weidick and Bennike, 2007
68º06′	50º02′	*Mya truncata* shell	4075±70	4123±214[a]	2.16	Ua-4583	Weidick and Bennike, 2007
68º06′	50º02′	*Odobenus rosmarus* tusk	4290±100	4441±322[a]	-13.05	Ua-2350	Weidick and Bennike, 2007
68º06′	50º02′	*Mya truncata* shell	5240±75	5614±178[a]	1.85	Ua-4579	Weidick and Bennike, 2007
68º06′	50º02′	*Balanus* sp.plate	5710±55	6118±140[a]	0.98	Ua-4578	Weidick and Bennike, 2007

All samples were recalibrated using Calib 6.0 which utilizes the updated INTCAL09 dataset

[a] Corrected for a marine resevoir effect of 400 years

Table DR4: Radiocarbon sample information

Core	Depth (cm)	Material Dated	Fraction Modern	Radiocarbon Age (^{14}C yr BP)	Calibrated Age (cal yr BP ± 2σ)	δ^{13}C (‰PDB)	Lab Number
09-ICE-5	23	aquatic macrofossil	0.9591±0.0015	335±15	390±80	-23.5	CURL-10083
09-ICE-5	36	aquatic macrofossil	0.7952±0.0019	1840±20	1770±60	-27.8	CURL-10439
09-ICE-5	57	aquatic macrofossil	0.6098±0.0015	3980±20	4470±50	-30.7	CURL-10434
09-ICE-5	70	aquatic macrofossil	0.4534±0.0013	6360±25	7300±120	-30.5	CURL-10441
09-ICE-3	45	aquatic macrofossil	0.9370±0.0013	525±15	530±20	-22.4	CURL-10081
09-ICE-3	95	aquatic macrofossil	0.5119±0.0009	5380±15	6200±80	-28.4	CURL-10093
09-NOR-3	23	aquatic macrofossil	0.7265±0.0010	2565±15	2680±60	-28.1	CURL-10089
09-NOR-3	74	aquatic macrofossil	0.5562±0.0010	4715±20	5450±130	-28.6	CURL-10091
09-NOR-3	103	aquatic macrofossil	0.4006±0.0008	7350±20	8160±120	-12.7	CURL-10092

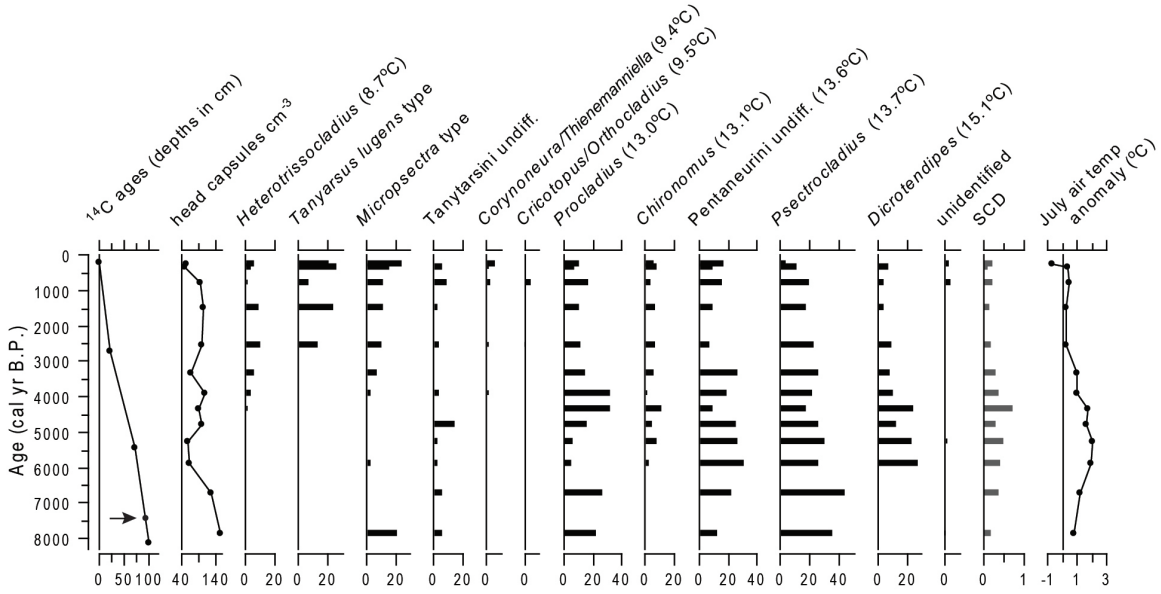

Figure DR1. Downcore data from sediment core 08-NOR-3, including chronology, head capsule concentrations, chironomid species percentages, squared-chord distance (SCD) of each sample from its closest analog in the training set, and chironomid-inferred July air temperatures (expressed as differences from the modern estimate obtained from chironomids in surface sediments). The age-depth model consists of three radiocarbon dates and an additional point at the surface representing present day. Arrow points to the likely onset of organic sedimentation (~7.4 ka) derived from nearby ^{10}Be ages and the basal radiocarbon age from Iceboom Lake.